A Dynamic Energy Budget simulation approach to investigate the eco-physiological factors behind the two-stanza growth of yellowfin tuna (Thunnus albacares)

E. Dortel, Laure Pecquerie, E. Chassot

Version of Record: https://www.sciencedirect.com/science/article/pii/S0304380020303677
Manuscript_5b4523d2f78394bb930ff7ee9da32961

A Dynamic Energy Budget simulation approach to investigate the eco-physiological factors behind the two-stanza growth of yellowfin tuna (*Thunnus albacares*)

E.Dortel[a,b,*], L.Pecquerie[c], E.Chassot[d,e]

[a] *Institut de Recherche pour le Développement (IRD), Avenue Jean Monnet, CS30171, 34203 Sète cedex, France*
[b] *MARBEC, Univ Montpellier, CNRS, Ifremer, IRD, Sète, France*
[c] *Univ Brest, CNRS, IRD, Ifremer, LEMAR, F-29280 Plouzané, France*
[d] *IRD, PO BOX 570, Victoria, Seychelles*
[e] *Seychelles Fishing Authority, PO BOX 449, Victoria, Seychelles*

Abstract

The growth of yellowfin tuna has been the subject of considerable research efforts since the early 1960s. Most studies support a complex two-stanza growth pattern with a sharp acceleration departing from the von Bertalanffy growth curve used for most fish populations. This growth pattern has been assumed to result from a combination of physiological, ecological and behavioral factors but the role and contribution of each of them have not been addressed yet. We developed a bioenergetic model for yellowfin tuna in the context of Dynamic Energy Budget theory to mechanistically represent the processes governing yellowfin tuna growth. Most parameters of the model were inferred from Pacific bluefin tuna using body-size scaling relationships while some essential parameters were estimated from biological data sets collected in the Indian Ocean. The model proved particularly suitable for reproducing the data collected during the Pacific yellowfin tuna farming experience conducted by the Inter-American Tropical Tuna Commission at the Achotines Laboratory in Panama. In addition, model predictions appeared in agreement with knowledge of the biology and ecology of wild yellowfin tuna. We used our model to explore through simulations two major assumptions that might explain the existence of growth stanzas observed in wild yellowfin tuna: (i) a lower food supply during juvenile stage in relation with high intra- and inter-species competition and (ii) ontogenetic changes in food diet. Our results show that both assumptions are plausible although none of them is self-sufficient to explain the intensity of growth acceleration observed in wild Indian Ocean yellowfin tuna, suggesting that the two factors may act in concert. Our study shows that the yellowfin growth pattern is likely due to behavioral changes triggered by the acquisition of physiological abilities and anatomical traits through ontogeny that result in a major change in intensity of schooling and in a shift in the biotic habitat and trophic ecology of this commercially important tuna species.

*Corresponding author
Email address: emmanuelle.dortel@cefe.cnrs.fr (E.Dortel)

Keywords: DEB theory, Body-size scaling, Behavioral changes, Ontogeny

1. Introduction

Yellowfin tuna (*Thunnus albacares*; YFT) is an epipelagic species widely distributed in the tropical and subtropical waters of the world's major oceans [52]. Owing to its high value as food source, YFT supports important commercial and recreational fisheries. With an annual global catch of about 1.3 million tonnes in the last decade, it ranks among the world's ten most harvested marine species [15]. At global scale, YFT has recently been assessed as Near Threatened following the Red list criteria of the International Union for Conservation of Nature [6], while the assessments of the status of its four oceanic stocks conducted within the tuna Regional Fisheries Management Organizations indicate that overfishing currently occurs in the Indian Ocean [28].

For assessment and management purpose, growth of wild YFT has been the subject of considerable research efforts since the 1960s through analysis of mark-recapture data, size frequency distribution of commercial fishery catches and ageing from calcified and bony structures [67, 9, 78]. YFT growth varies between ocean basins and regions and shows in some areas some complex pattern that departs from the traditional von Bertalanffy growth curve used for most fish stocks [52]. In particular, some growth studies conducted in the Atlantic, Indian and Western-Central Pacific Oceans support a two-stanza growth pattern with a sharp acceleration in growth rate at about 60-65 cm fork length [23, 36, 11, 14].

The complex growth pattern observed in some populations of YFT has been assumed to result from a combination of physiological, ecological and behavioral factors but the role and contribution of each of them have not been addressed yet [18, 2, 22, 11]. A better understanding of these mechanisms is essential to assess the plasticity of YFT growth and eventually strengthen the scientific advice on the stock status and improve the overall quality of current stock assessments.

We investigated the factors governing the growth of YFT with a bioenergetic model that covers the different post-metamorphic life stages of the Indian Ocean YFT within the framework of the Dynamic Energy Budget (DEB) theory [35]. DEB theory has already proven successful to study growth and reproduction of a large range of marine taxa [75, 70, 53, 21] and more recently to study the dynamics of populations and ecosystems [45, 55, 44]. Other bioenergetic approaches are available but they are generally specific to a particular life stage and unsuitable for modelling the changes between distinct life stages [26, 49]. In contrast, the DEB theory provides a powerful conceptual framework to describe the lifelong growth in relation to other physiological requirements, such as metabolism and body internal maintenance, development and reproduction, as a function

of environmental food conditions and organism state [35, 21].

2. Materials and methods

2.1. Data sources

We collected data sets from the literature for both wild and farmed YFT to compare the outputs of the bioenergetic model with morphometric, ageing and reproduction observations.

2.1.1. Wild Indian Ocean yellowfin tuna

For wild YFT, we considered a length-at-age data set collected throughout the Regional Tuna Tagging Project (RTTP), a large scale mark-recapture program conducted in the Western Indian Ocean between 2005-2007, and the West Sumatra Tuna Tagging Project (WSTTP), a tagging program conducted off the western Indonesian coast in August 2007 [1, 48]. All lengths were measured with a measuring board to the nearest 0.1 cm in fork length (L_F), i.e. the projected straight distance measured from the tip of the upper jaw to the shortest caudal ray. Fish ages were estimated from readings of saggital otoliths collected from (i) 128 YFT caught through the RTTP and measuring between 43-72 cm L_F at tagging and 47.9-135.4 cm L_F at recapture, (ii) 18 fish caught through the WSTTP measuring between 19-29 cm L_F, (iii) 35 fish, including 7 females, collected from 2008-2009 at the Indian Ocean Tuna Ltd. cannery and measuring between 31-147.5 cm L_F [47, 64]. Otoliths were prepared for age analysis and read at the "Laboratoire de Sclérochronologie des Animaux Aquatiques" (Brest, France) following the method described by Stéquert [72]. The number of otolith growth increments was counted repeatedly for different otolith sections [47, 64]. The ages were estimated from these counts using an ageing error model that explicitly accounts for process and interpretation errors in otolith readings [10].

We also considered length-weight measurements from defrosted YFT caught in the whole Indian Ocean basin. Fork length was measured with a caliper to the nearest 0.1 cm and total weight was measured with a scale to the nearest 0.1 kg [4]. The data set included: (i) 5,089 fish from the Indian Ocean Tuna Ltd. cannery caught during 2005-2012 (66-165 cm L_F, 5.8-87.5 kg) and (ii) 100 additional fish collected in 2010-2013, of which 35 females (54.7-148.2 cm L_F, 3.4-61.5 kg) and 65 individuals whose sex was indeterminate (29-61 cm L_F, 0.4-4.1 kg).

Finally, we used a data set of batch fecundity, i.e. number of eggs released per batch, derived from gravimetric method applied to 40 YFT females in the size range 79-146.9 cm L_F that were collected on board commercial purse seiners in the western Indian Ocean during 2009-2010 [79]. The batch fecundity varied from 0.32 million to 6.91 million eggs with a mean of 3.07 million eggs.

2.1.2. Farmed Pacific yellowfin

We used data from YFT farming experiment conducted by the Inter-American Tropical Tuna Commission (IATTC) in Achotines Laboratory in the Republic of Panama [76]. This experiment lasted over 3 years and involved 55 YFT (53% females, 46% males) caught in the coastal waters of the northwest Panama Bight, in 1996 and 1998, and then transferred in a broodstock YFT tank. The tank was filled with seawater and semi-open to ocean, thus the temperature and salinity in tank were influenced by the seasonal fluctuations in ocean upwelling and rainfall. During the experiment, daily temperatures in tank ranged from 20.1 to 29.7°C with an average of 27.5°C. YFT were fed once per day with one of five prey species whose caloric values were calculated based on metabolizable energy values of protein (17.7 kJ.g^{-1}) and lipid (33.5 kJ.g^{-1}). The length and wet weight of fish were measured at the time of the transfer in the tank and at their death. The food daily rations (FDR, % body wet weight day) are also available from the literature [76]. They were calculated as the ratio between the wet weight of ingested food and the wet weight of an individual at each time step t of the simulation, i.e. 1 day. A food conversion ratio (FCR) was estimated as the ratio between the wet weight of ingested food on increasing biomass over given times intervals of 12–103 days for a constant number of YFT.

2.2. Description of the yellowfin tuna DEB model

2.2.1. State variables and dynamics

The yellowfin life cycle includes five different stages: embryo, larva, early juvenile, juvenile and adult. In this study, we implemented a bioenergetic model based on DEB theory [35] that only describes three life stages of YFT: early juvenile, juvenile and adult. This model was focused on an individual fish defined by four state variables: reserve (E in J), structural length (L_V in cm), maturation (E_H in J) and reproduction (E_R in J). Instead of the dynamics of the reserve E, we followed the dynamics of the scaled reserve density e which is driven by the dynamics of E. The scaled reserve density $e = [E]/[E_m]$ is a dimensionless quantity where $[E] = E/L_V^3$ is the reserve density and $[E_m]$ represents the maximum reserve density.

The four state variables and the parameters used are described in the Table 2. The dynamics of the state variables (Figure 1) are controlled by various energy fluxes varying with size and body temperature (Table 3). The energy derived from ingested food is directly assimilated into the reserve ($\dot{p}_A$). From there, the energy is mobilized according to the κ-rule. A constant fraction (κ) is allocated to somatic maintenance ($\dot{p}_S$) and growth ($\dot{p}_G$), with priority for somatic maintenance. The rest is allocated to maturity maintenance ($\dot{p}_J$) and maturation or reproduction in adults ($\dot{p}_R$), with priority for maturity maintenance. Maturation explicitly refers to the fish development and the transitions from one stage to another occur for defined maturity thresholds, E_H^e from early

juvenile to juvenile and E_H^p from juvenile to fully developed adult.

The beginning of the juvenile stage is marked by the acquisition of thermoconservation ability, a notable property of most tuna species compared to other fish species [5]. From about 20 cm L_F, YFT is able to raise the temperature in some parts of its body above the seawater temperature by the storage of the metabolic heat through vascular heat exchanger systems [77, 68]. We assumed that the thermoconservation ability of YFT involved energetic costs proportional to the square of structural length. The initiation of the thermoconservation ability occurs as a point in time once E_H reaches E_H^e (Eq. D2 in Table 2). This assumption slightly simplifies the model compared to the DEB-based model developed for Pacific Bluefin tuna (*Thunnus orientalis*) which considered a gradual increase of the energetic costs associated with regional endothermy [31].

Once at the adult stage, the maturity level does not increase any further and the fish stores energy in a reproduction buffer throughout the year. During a spawning season, the energy stored in the reproduction buffer is converted to eggs according to species-specific handling rules. Two spawning seasons are observed, a main season from November to March and a second minor period in June-July [73, 79]. As observed for Pacific YFT, we considered that spawning is triggered when water temperature reaches 24°C and ends above 28°C [29, 40]. Spawning was considered to occur almost daily from December-March and June-July and for seawater temperatures between 24°C and 28°C when the reproduction buffer contains sufficient energy to produce a batch.

Consistent with the multiple batch spawning behaviour of YFT, the energy stored in reproduction buffer is released through several batches with an increasing energy requirement per batch as fish grows. The energy required to produce one batch (E_B in J) includes the energy content of eggs and energy losses to convert the energy of reproduction buffer into yolk material:

$$E_B = \frac{[E_B] L_V^3}{\kappa_R} \tag{1}$$

where $[E_B]$ is the energy density of one batch (J.cm^{-3}). The number of eggs released per batch (N_B) can be estimated from the energy requirement per batch and the energy content of one egg (E_0) following:

$$N_B = \frac{E_B}{E_0} \tag{2}$$

where E_0 was estimated to have a mean value of 1.295 J based on the mean dry weight of an egg of captive yellowfin (about 0.043 mg; [40]) and the lipid contents of the eggs of wild Atlantic bluefin tuna (*Thunnus thynnus*) and bonito (*Sarda sarda*) estimated to be 7.953 J.mg^{-1}, i.e. 26.4% of the total caloric value of a freshly spawned egg or approximately 20% of its dry mass [51].

2.2.2. Forcing variables

Consistent with DEB theory, two forcing variables were considered, the body temperature T (K) and the food density X (J.m^{-3}). Body temperature affects all the metabolic fluxes including the maximum assimilation $\{\dot{p}_{Am}\}$, the somatic maintenance rates $[\dot{p}_M]$ and $\{\dot{p}_T\}$ as well as $\dot{v}$ and $\dot{k}_J$. The values of those rates fluctuate within a species-specific tolerance range as described by the Arrhenius relationship. Let $\dot{k}(T)$, the value of a metabolic rate $\dot{k}$ at any temperature T (K), T_A the species-specific Arrhenius temperature (K) and T_1 a chosen reference temperature (K):

$$\dot{k}(T) = \dot{k}(T_1)\, \exp\left(\frac{T_A}{T_1} - \frac{T_A}{T}\right) \tag{3}$$

The food density is converted into ingestion according to a Holling type II scaled functional response, a dimensionless quantity defined as:

$$f = \frac{X}{X + X_k} \tag{4}$$

X_k, the half-saturation constant, is the food density for which the ingestion rate is half its maximum value [35].

2.2.3. Link between state variables and fishery observations

The DEB state variables cannot be measured directly, only indirectly with additional assumptions to relate these state variables with the observations such as length, weight and fecundity. The structural length L_V is related to the physical length expressed in fork length L_F (cm) using the species-specific shape coefficient δ_j:

$$L_F = \frac{L_V}{\delta_j} \tag{5}$$

The wet weight W_W (g) has contributions from structure W_V, reserve W_E and also from reproduction buffer for adults W_{E_R} and it expresses as follows:

$$W_W = W_V + W_E + W_{E_R} = d_V L_V^3 + \frac{E + E_R}{\rho_E} \tag{6}$$

where d_V is the density of the structural volume (g.cm^{-3}) and ρ_E is the energy content per gram of reserve or reproduction buffer.

We also define the reproductive investment I_R as the ratio between the weight of reproduction buffer and the wet weight of fish. This latter provides information on the weight losses due to the spawning activity.

$$I_R = 100 \times \frac{W_{E_R}}{W_W} = 100 \times \frac{E_R}{d_V \rho_E L_V^3 + E + E_R} \tag{7}$$

2.3. Model calibration

Body-size scaling relationships provide rules for how primary parameters vary among phylogenetically related species [35]. The intensive parameters are related to biochemical processes and they are assumed roughly invariant among related species, while the extensive parameters ($\{\dot{p}_{Am}\}$ and maturity thresholds) depend on maximum size [35, 50]. Thus, the extensive parameters can be directly adjusted using a zoom factor z defined as the ratio of the maximum structural length of species of interest to that of the reference species.

Our model is very close to the model developed for Pacific Bluefin Tuna (PBT) [31], with a slight difference in the energetic process related to the acquisition of thermoconservation ability. In both models, this acquisition resulted in an additional energy cost which gradually increases from metamorphosis until the end of the early juvenile stage for Jusup et al. [31] while this additional cost appears at the end of the early juvenile stage in our model. Thus, the parameters of adult PBT were used as a first approximation of primary parameters. First, the body-size scaling relationships were used to infer the values of the surface-area specific maximum assimilation rate $\{\dot{p}_{Am}\}$ and the maturity thresholds E_H^j, E_H^e and E_H^p from those of PBT. Under constant food and temperature conditions, the maximum structural length can be related to the physical asymptotic length L_{F_∞}. Thus, the maximum structural length of YFT was estimated from an asymptotic length fixed to 200 cm L_F as follows:

$$L_m = \frac{\delta_j L_{F_\infty}}{f} \tag{8}$$

Then the shape parameter δ_j, the structural volume density d_V and the weight-energy coupler ρ_E, can be estimated from the length-weight relationship of juveniles. As juveniles do not store energy for reproduction, the wet weight (W_W) can be expressed from the physical length and the reserve density $[E] = E/L_V^3$ (J.cm^{-3}) as follows:

$$W_W = \left(\delta_j^3 L_F^3 \left(d_V + \frac{[E]}{\rho_E}\right)\right) \tag{9}$$

This length-weight relationship was fitted to data of wild immature YFT including 87 fish measuring 29-61 cm and weighing 0.39-4.2 kg in a Bayesian framework. Without prior knowledge, an uninformative inverse gamma distributions was assigned to $[E]$. d_V was assigned a normal distribution centered on 1. δ_j was assumed to vary according to a beta prior distribution between 0 and 1. ρ_E was fixed such that the ratio of ρ_E to δ_j was the same as in Jusup et al. [31]. The parameters estimate was based on sampling approach of Markov Chain Monte Carlo simulations as implemented in OpenBugs version 3.2.1 [71]. Three MCMC chains of 100,000 samples, thinned to one draw every 1000^{th} sample, were used to estimate the parameters. The convergence to the

stationary posterior distribution was assessed by the Gelman-Rubin diagnostic from the second half of MCMC simulation sample [24].

The Arrhenius temperature T_A was deduced from the value of the van't Hoff coefficient Q_{10} estimated for juveniles Pacific YFT, i.e. 1.65 at 18-24°C and 1.67 at 24-30°C [8]. The Q_{10} is a correcting factor applied to metabolic rates for every 10°C increase in temperature. For any body temperature T, Q_{10} and T_A are related according to the following relationship:

$$Q_{10} = \exp\left(\frac{10T_A}{T(T+10)}\right) \tag{10}$$

The maturity thresholds, E_H^j, E_H^e and E_H^p were adjusted such that the corresponding physical lengths are consistent with available knowledge from literature. The metamorphosis of YFT occurs at about 13 mm standard length (S_L) [32], the end of early juvenile stage corresponds to a size of 20 cm L_F [77] and the puberty to a size close to 75 cm L_F [79].

Finally, the energy density for a single batch [E_B] was estimated from the relationship between the fork length and the batch fecundity observed for wild YFT.

2.4. Model validation using simulation

Different simulations were performed to assess the model suitability. Firstly, the model was used to simulate the growth in length, the length-weight relationship, the food daily ration (FDR) and the food conversion ratio (FCR). The simulation outputs were then compared to the observations described in the study of Wexler et al. [76]. The FDR (% body wet weight per day) was calculated as the ratio between wet weight of ingested food W_X and the wet weight of an individual W_W at each time step of the simulation, i.e. 1 day. At any time t:

$$FDR = 100 \times \frac{W_{X_t}}{W_{W_t}} \tag{11}$$

The FCR was calculated as the ratio between the wet weight of ingested food and increased wet weight of an individual over time interval of 1 day ignoring the weight of the reproduction buffer:

$$FCR = \frac{W_{X_{t-1}}}{(W_{v_t} + W_{E_t}) - (W_{v_{t-1}} + W_{E_{t-1}})} \tag{12}$$

The wet weight of ingested food at time t was calculated using the following equation:

$$W_{X_t} = \frac{f\{\dot{p}_{Am}\}L_{v_t}^2}{\kappa_X \rho_X} \tag{13}$$

ρ_X is the energy content of 1 g of food estimated from the caloric value of prey given in Wexler et al.

[76]. As the prey provided to farmed YFT for a given day was not specified, three values illustrating the range of possible levels in terms of energy were used for ρ_X. These values corresponded to the most energetic species (6471 J.g^{-1}), the less energetic species (2980 J.g^{-1}) and the mean (4910 J.g^{-1}).

This first simulation was performed for a constant food density expressed through a scaled functional response $f = 0.925$ and for body temperatures considered equivalent to the daily temperatures in the experimental tank [76]. The age and length at the experiment start were considered as initial conditions, i.e. an age of 395 days and a length of 53 cm L_F from which we deduced a structural length $L_V = 13.53$ cm and a maturity level $E_H = 2,460,526$ J.

The seasonal reproductive investment (I_R, Eq. 7) was explored with another simulation. This latter simulation was run under constant body temperature of 27°C and constant food density ($f = 0.925$) from metamorphosis to fish death. The initial state of the system agreed with the fish state at metamorphosis, i.e. a maturity level E_H^j, age of 30 days and fork length of 1.3 cm from which we deduced a structural length of 0.33 cm.

Both simulations were performed with a 1-day time step using the *dde* function, a numerical solver for delay differential equations implemented in the *PBSddesolve* package [7] of the R software [61].

2.5. Investigating eco-physiological factors behind the growth stanzas

In this section, we investigated through simulations two main assumptions that could explain the growth stanzas observed in wild YFT: (i) a decrease of competition for food resource due to change in schooling behavior and (ii) a change in food diet due to habitat change in relation with the improvement of some physiological traits. For both assumptions, the growth in length was simulated with a 1-day time step, under constant temperature of 27°C from metamorphosis to fish death. The average annual growth rates by 10 cm size-class, from 20 to 90 cm, were computed and compared to those of wild Indian Ocean YFT as estimated by Dortel et al. [11] with otolith data and otolith and length-frequency data. The relative root mean square error (RMSE), a normalized indicator that measures the discrepancy between the average annual growth rates simulated (r^*) and estimated for wild Indian Ocean YFT (r) was used:

$$RMSE = \frac{\sqrt{(r^* - r)^2}}{r^*} \tag{14}$$

2.5.1. Competition for food resource

Juveniles of YFT form mixed schools with juveniles of bigeye and skipjack under floating objects such as the fish aggregating devices (FADs) deployed in purse seine fisheries to increase fishing

success [20]. Within the schools, the inter- and intra-species competition for food resource is assumed to be strong which could result in lower food intake by young YFT as compared to adults [58, 25, 65]. In our simulations, this was expressed by a lower value of food density modeled through a lower scaled functional response below 70 cm L_F which corresponds to the size at which YFT leave the schools associated with floating objects [20]. Two functional responses, f_j and f_p for juvenile and adult stages, respectively, were defined such that $f_j < f_p$ and the effect of an abrupt transition from f_j to f_p was investigated. Four values of f_j were tested, 0.8, 0.825, 0.85 and 0.875, for a value of f_p fixed to 0.925.

2.5.2. Food diet change

In the Indian Ocean, YFT feed on a wide variety of epipelagic and mesopelagic fish, crustaceans and cephalopods and their diet varies according to size and foraging depth [39, 59, 80]. Adult YFT are dispersed over a wider geographical area covering deeper and colder waters and, contrary to juveniles, they can dive below the thermocline to forage [66]. Thus, juveniles might have access to a range of prey which might be not as nutritious as for adults. This was expressed in our simulations through a lower surface-area specific maximum assimilation rate for YFT smaller than 60 cm L_F, the minimum size of fish exhibiting deep dives [66]. Two assimilation rates, $\{\dot{p}_{Am}\}_j$ and $\{\dot{p}_{Am}\}_p$, were defined for juveniles ans adults respectively such that $\{\dot{p}_{Am}\}_j < \{\dot{p}_{Am}\}_p$ and the effect on growth of an abrupt transition from $\{\dot{p}_{Am}\}_j$ to $\{\dot{p}_{Am}\}_p$ was investigated. We considered two values of $\{\dot{p}_{Am}\}_j$, 3900 and 4000 J.day^{-1}.cm^{-2}, for a value of $\{\dot{p}_{Am}\}_p$ fixed to 4370 J.day^{-1}.cm^{-2}.

3. Results

3.1. Validation of a reference DEB model for yellowfin tuna

The reference DEB model successfully reproduced the growth in length and the length-weight relationship observed for farmed Pacific YFT as described in the study of Wexler et al. [76]. Furthermore, the observed values of FDR and FCR were well within the simulated range (Figure 2). Thus, the set of parameters, some of which were derived from PBT [31], appeared suitable to assess the effects of variations in the quantity and quality of food on YFT growth (Table 1).

From the length-weight relationship for immature YFT, the value of d_V was estimated to be significantly higher than 1 (Table 4). This is in agreement with the observation that tuna have a higher density than seawater [38]. The value of ρ_E was found to be lower than for PBT, reflecting a lower energetic value for YFT due to a lower mass of red muscle.

From the Q_{10} values observed for juvenile YFT in Pacific Ocean, the Arrhenius temperature was estimated at 4622 $\pm$ 207 K. This value was lower than that of PBT estimated at about 5298 K,

which could indicate that YFT are less sensitive to temperature variations within their temperature tolerance range, although more temperature data would be required to validate this assumption.

3.2. Yellowfin growth according to the reference DEB model

For a constant temperature of 27°C and a constant food density f=0.925, the reference DEB model forecasted particularly fast growth until the end of the early juvenile stage. Then, it predicted a Von Bertalanffy type growth. Regarding wild Indian YFT, the model appeared suitable for adult growth but overestimated juvenile growth (Figure 3.A). The puberty was reached at a length of abour 75 cm corresponding to an age of 1.4 years. The evolution of weight relative to length was higher than expected, which may indicate a too high level of food density (Figure 3.B).

The energy stored in the reproduction buffer was also converted in weight to determine the seasonal reproductive investment. This latter increased with fish size up to 27.8% of total body wet weight for fish of 89 kg (150 cm L_F) and then slightly decreased to 25.9% of body wet weight (Figure 4).

3.3. Effect of food density

A decrease in food supply during the juvenile stage resulted in lower growth rates, from 20% to 60% depending on the f values. For a value between 0.825 and especially 0.85, the model predicted a two-stanza growth which better captured the juvenile growth, leading to 52-71% and 81-87% decrease in RMSE values between 30-70 cm compared to the reference model (Table 5). But as shown in Figure 5.A, the model underestimated the magnitude of growth acceleration. The age at puberty increased at 1.83, 2.11, 2.5 and 3.14 years for a decrease in f from 0.875 to 0.8, while the fork length at puberty remained almost constant and varied around 74.9 cm.

3.4. Effect of prey quality

A reduced energy intake in young YFT led to an average decrease in the growth rate of 37% and 29% for $\{\dot{p}_{Am}\}_j$ values of 3900 and 4000 J.day^{-1}.cm^{-2} respectively. For both values, the model was able to capture the juvenile growth, as shown by the 66-72% and 86-87% decrease in RMSE values between 30-60 cm (Table 5), but it underestimated the magnitude of growth acceleration (Figure 5.B). The predicted age and fork length at puberty were 2.2 years for 74.79 cm and 1.96 years for 74.77 cm for $\{\dot{p}_{Am}\}_j$ values of 3900 and 4000 J.day^{-1}.cm^{-2} respectively.

4. Discussion

We formulated a bioenergetic model covering the juvenile and adult stages of YFT in the context of Dynamic Energy Budget theory. Some essential parameters of the model were estimated with Bayesian analysis from morphometric, age, and reproduction data sets collected from YFT sampled in the Indian Ocean while other parameters were derived from the DEB model developed for PBT

[31]. Our results show that both lower food availability in the juvenile stage and ontogenetic changes in food diet characterized by the consumption of more energetic prey in older fish can explain the complex two-stanza growth observed in wild but not captive YFT. Both assumptions could explain the growth acceleration observed in wild YFT but none of them was self-sufficient to reflect the level of change observed. We thus assumed that the observed acceleration resulted from a combination of both processes.

4.1. Yellowfin DEB model

DEB theory allows to describe continuously growth and reproduction over the organism lifespan [50]. Hence, DEB theory appeared as a particularly suitable framework for the study of YFT growth throughout different life stages. However, the experimental data currently available on YFT physiology are insufficient for estimating a comprehensive set of parameters. It was however possible to benefit from the work on PBT through the use of the body-size scaling relationships [35, 54]. Under these relationships, YFT and PBT have similar metabolic and physiological processes and the differences between the two species would mainly result to lower energy assimilation for YFT. This assumption may not be quite accurate. Indeed, bluefin tuna have greater abilities for conservation of metabolic heat due to more developed vascular heat exchanger systems and a higher proportion of red muscle resulting in a more extensive thermal-niche than YFT [3, 68]. As the internal heat production is scaled with the surface, the surface area-specific maintenance costs, $\{\dot{p}_T\}$, are probably lower for YFT. Despite that, the set of parameters approximated from primary parameters of PBT has proved particularly suitable for reproducing the experiments on captive YFT and the model predictions appeared in agreement with the knowledge of the species biology.

In constant conditions of temperature and food, the reference model forecasted particularly fast initial growth until the end of the early juvenile stage. Then, as was expected for farmed fish, it complied with a Von Bertalanffy growth, with relatively high growth rates for juveniles and young adults which gradually slowed as asymptotic length approaches. The warming ability of tissues from retention of metabolic heat appears toward the end of the early juvenile stage [68]. According to our assumption, this ability is associated with an additional somatic maintenance cost and it led to a change in the energy balance resulting in a growth slowdown.

Regarding wild YFT, the growth pattern predicted by the reference model was consistent with the adult growth over 90 cm L_F but it overestimated growth in juvenile and pre-adult stages. Therefore, the puberty was reached at a length of about 75 cm L_F, consistent with observations of length at maturity in the Indian Ocean [75 - 90 cm 62, 79], but at 1.4 years, an earlier age than expected by the growth model of Indian Ocean YFT [2.2-2.5 years 11]. By contrast, the predicted length-weight relationship appeared suitable for juveniles, but the model overestimated the

weight gain over 100 cm L_F, suggesting an excessive weight contribution of the reproduction buffer.

4.2. Growth and population dynamics

A comparison of the biological parameters used in population dynamics models shows major differences in growth pattern and rates between the four world stocks of YFT [52]. The plasticity in tuna growth has generally been attributed to differences in oceanographic parameters (e.g. sea temperature) and prey availability [e.g. 12] and the environment and oceanic food webs that support YFT vary substantially across oceans and regions [56]. The availability of data sources and choice of estimation method may, however, also modify the growth models and affect our perception of tuna growth [34].

In the Indian Ocean, historical and recent studies based on multiple data sources support a marked two-stanza growth pattern with a sharp acceleration in growth rate at about 60-65 cm fork length [42, 11, 14]. In the Atlantic Ocean, the two-stanza growth model derived in the early 1990s from length-frequency data and used for several assessments of the stock status of YFT [23] has been challenged by direct age estimates from counts of daily growth increments in sagittal otoliths that support a von Bertalanffy growth curve [69]. Results from otolith reading however appear inconsistent with the maximum length of Atlantic YFT and growth rates derived from past tagging programs conducted by the International Commission for the Conservation of Atlantic Tunas, calling for further studies integrating information from multiple data sources in this ocean [19]. Recent mark-recapture data collected in the Atlantic Ocean indicate that tagged fish released with lengths of less than 65 cm tend to grow slower than expected from a von Bertalanffy model while fish above 65 cm tend to grow faster, a pattern modelled with a Richards growth curve in the most recent assessment of Atlantic YFT [27]. As part of the Atlantic Ocean Tropical Tuna Tagging Program, some work is ongoing to develop an integrated growth model accounting for the new data set collected on YFT growth.

Tropical tuna growth is the major focus of current research in the Pacific Ocean [16]. In the Western-Central Pacific Ocean, the growth model used for assessing the stock of YFT predicts a growth rate slowing between about 40 and 70 cm, similarly to that observed in the Indian Ocean [36, 74]. Changes in configuration of the YFT population model also suggest some regional differences in estimated growth rates consistently with direct age estimates and mark-recapture experiments [74]. Preliminary results from annual increment counts in otoliths suggest that the degree of two-stanza might however be lower than previously considered [17]. In the Eastern Pacific Ocean, the stock of YFT shows a more classical growth pattern than that observed in the other ocean basins [46]. The ageing technique based on daily increment counts for this stock has however recently been

challenged [17]. Ongoing research focusing on annual increments in otoliths is expected to shed the light on the growth of the two stocks of Pacific YFT.

4.3. Behavioral changes behind the two-stanza growth

According to the experiment of Wexler et al. [76], farmed YFT did not exhibit the growth acceleration occurring around 65 cm L_F for wild fish. Similarly to the experiment of Achotines, the growth pattern of YFT held in captivity for several years at the Tuna Research and Conservation Center (TRCC) in Pacific Grove, California is well described by a von Bertalanffy model [13]. In this experiment, YFT were however found to grow significantly slower than those of the IATTC experiment. These observations supported that the origin of the stanza growth would rather be behavioral or ecological than physiological. In captivity, the food intake is adjusted to comply with the nutritional requirements of tunas which do not suffer from competition for food. Thus, the growth stanza would be caused by a behavioral change related to feeding. Indeed, both assumptions, i.e. a low food availability and the consumption of less energetic prey during the juvenile stage, led to a two-stanza growth with growth acceleration in relation with behavioral change. For a decrease in food density X from 54% to 62% or a reduction in the assimilation rates from 8.5% to 10.75%, the model captured the juvenile growth but the intensity of growth acceleration and overall adult growth were underestimated. In addition, YFT reached puberty at similar sizes as those predicted by the reference model but at older ages, leading to age values in better agreement with those expected, i.e. between 2.2 and 2.5 years according to the growth curve of Indian Ocean YFT [11].

Several lines of evidence support low feeding rates for juveniles of YFT when they occur in mixed schools associated with drifting objects. In particular, stomach contents analysis point out to a much higher proportion of empty stomachs for fish caught from associated schools which are significantly slimmer than YFT caught in free swimming schools [58, 25, 30]. This might be explained by the high level of intra-species competition and decreased foraging success in YFT when they occur in large schools [44].

YFT is an opportunistic species that feeds on a large number of prey categories and trophic studies underline a change in diet with size as well as the ability of larger YFT to forage in deeper waters [59, 60]. Firstly, YFT feed mainly on planktonic crustaceans and then, from 50 cm L_F, they become essentially piscivorous, with a decline in crustaceans consumption and a strong consumption of cephalopods between 80-100 cm [39, 58]. Recent analysis of fatty acids and stable isotopes of carbon and nitrogen showed some major ontogenetic changes in the diet of Indian Ocean YFT [65]. In particular, the shift in concentration of neutral fatty acids observed in the liver of YFT

at around 70-80 cm might reflect the change of habitat from surface to deeper layers where rich-MUFA prey of YFT such as myctophids and their predators are more abundant [65]. Investigating the caloric value of prey found in YFT stomach contents at various size classes would be useful to quantitatively assess the energetic contribution of each prey group to the ontogenetic changes in diet.

4.4. Variability in YFT growth

Most tuna stock assessments assume a constant individual growth described with some individual variability around the mean [34]. Changes in population abundance and environmental conditions may however affect growth rates over space and time as evidenced for southern bluefin tuna [37, 57]. Growth parameters used for the assessment of Indian Ocean YFT are considered constant over almost seven decades when the stock has experienced a strong decline in abundance [28] and YFT fishing grounds have been characterized by major temporal changes in temperature and primary productivity [63]. Furthermore, the increasing use of FADs to aggregate juveniles of YFT and skipjack tuna since the early 1990s might have increased intra and inter-species competition and led to changes in growth rates [43, 25]. Assessing the influence of FAD density on YFT growth is very difficult due to the lack of routine monitoring for ageing tunas linked to the high costs and logistics of sampling and otolith reading. Developing standard ageing procedures across tuna RFMOs with otolith reference collections constitutes a first step to monitor changes in age-length relationships and promote the comparison of tuna growth between oceans [64, 17]. In addition, we recommend the systematic implementation of comprehensive ageing projects in conjunction with large-scale tagging programs every five or ten years to track changes in growth rates and better account for growth variability in the demographic analysis of these socio-economically important species.

5. Conclusion & perspectives

Building on the Dynamic Energy Budget modelling framework that mechanistically links the biology of individual organisms to abiotic drivers [35], our model suggests that the unique growth pattern observed in wild YFT could stem from a major change in intensity of schooling and associative behavior with size, which would substantially modify both the quantity and quality of food available for maintenance, reproduction and growth. This change would be triggered by the acquisition of physiological abilities and anatomical traits with age and result in an ontogenetic shift in the biotic habitat and trophic ecology of YFT. In addition, the intensity of schooling might depend on population abundance, with higher density resulting in the formation of larger schools described by a higher degree of competition [45, 44].

Next steps of the work will include the development of a comprehensive calibration and sensitivity analysis to identify the most influential parameters of the model and estimate the ranges of values driving different shapes of growth curves and the associated age-length keys that are used for assessing the status of YFT stocks. To this end, the data collected at TRCC would be useful to estimate a comprehensive set of parameters as well as to disentangle the relative contributions of water temperature and low energy diet on the low growth rates of YFT observed at TRCC. More generally, tuna morphometric and bioenergetic data collected for scientific purpose under controlled environmental conditions are extremely difficult and costly to obtain [32, 33, 13, 41]. Making such valuable information available and accessible (e.g. with standard metadata) would foster their use as inputs for models and make the most of the data.

Acknowledgments: This study was funded by the European Union (Reg.199/2008, 665/2008 and SI2.604453), the French Ministry of Agriculture and Fisheries (301629/00), ORTHONGEL, the Institut de Recherche pour le Développement, and the French ANR funded project EMOTION (ANR 11JSV7 007 01). We wish to acknowledge the contributions of all the people who have been involved in the Regional Tuna Tagging Project of the Indian Ocean, funded under the 9^{th} European Development Fund (9.ACP.RSA.005/006) of the European Union and the West Sumatra Tuna Tagging Project funded by the Government of Japan. We are grateful to F Sardenne, G Le Croizier, E Morize, JM Munaron, C Geffroy and E Dabas for their contribution to otolith analysis, M Herrera, C Assan, and A Delgado de Molina for data on YFT size measurements, and P Dewals and his team for their work on recoveries and sex identification. We particularly thank M Jusup for his help with the code of the PBT model and I Zudaire for advice on YFT spawning behavior. The manuscript benefited from fruitful discussions with O Maury, D Margulies, N Bodin, F Sardenne, D Gaertner, A Fonteneau, O Gimenez, N Bousquet and M Huret. We finally thank the reviewers for their useful comments that greatly improved the manuscript.

References

[1] Anonymous (2008) West Sumatera Tuna Tagging Project 2006-2007, Final Report. Tech. rep., Indian Ocean Tuna Commission

[2] Bard F (1984) Croissance de l'albacore (*Thunnus albacares*) Atlantique d'après les données des marquages. Collective Volume of Scientific Papers ICCAT 20(1):104–116

[3] Blank JM, Farwell CJ, Morrissette JM, Schallert RJ, Block BA (2007) Influence of swimming speed on metabolic rates of juvenile pacific bluefin tuna and yellowfin tuna. Physiological and Biochemical Zoology 80(2):167–177. URL `https://www.journals.uchicago.edu/doi/abs/10.1086/510637`

[4] Bodin N, Chassot E, Sardenne F, Zudaire I, Grande M, Dhurmeea Z, Murua H, Barde J (2018) Ecological data for western Indian Ocean tuna. Ecology 99(5):1245–1245. URL https://esajournals.onlinelibrary.wiley.com/doi/abs/10.1002/ecy.2218

[5] Brill RW (1994) A review of temperature and oxygen tolerance studies of tunas pertinent to fisheries oceanography, movement models and stock assessments. Fisheries Oceanography 3(3):204–216

[6] Collette BB, Reeb C, Block BA (2001) Systematics of the tunas and mackerels (Scombridae). In: Tuna physiology, ecology and evolution, Academic Press, vol. 19 of *Fish Physiology Series*. 1–33

[7] Couture-Beil A, Schnute J, Haigh R (2010) PBSddesolve: solver for delay differential equations. rpackage version 1.08.9

[8] Dewar H, Graham J (1994) Studies of tropical tuna swimming performance in a large water tunnel - Energetics. Journal of Experimental Biology 192(1):13–31. URL http://jeb.biologists.org/content/192/1/13

[9] Diaz E (1963) An increment technique for estimating growth parameters of tropical tunas, as applied to yellowfin tuna (*Thunnus albacares*). Inter-American Tropical Tuna Commission Bulletin 8(7):383–416

[10] Dortel E, Massiot-Granier F, Rivot E, Million J, Hallier J, Morize E, Munaron J, Bousquet N, Chassot E (2013) Accounting for age uncertainty in growth modeling, the case study of yellowfin tuna *Thunnus albacares* of the Indian Ocean. PLoS ONE 8(4):1–12. URL http://journals.plos.org/plosone/article?id=10.1371/journal.pone.0060886

[11] Dortel E, Sardenne F, Bousquet N, Rivot E, Million J, Le Croizier G, Chassot E (2015) An integrated Bayesian modeling approach for the growth of Indian Ocean yellowfin tuna. Fisheries Research 163:69–84. URL http://www.sciencedirect.com/science/article/pii/S0165783614002203

[12] Dueri S, Maury O (2010) Application of the APECOSM-E model to the skipjack tuna (*Katsuwonus pelamis*) fisheries of the Indian Ocean. In: IOTC Proceedings. IOTC, Victoria, Seychelles, 18-26 October 2010, vol. IOTC-2010-WPTT12-17, 36p

[13] Estess EE, Klinger DH, Coffey DM, Gleiss AC, Rowbotham I, Seitz AC, Rodriguez L, Norton A, Block B, Farwell C (2017) Bioenergetics of captive yellowfin tuna (*Thunnus albacares*). Aquaculture 468:71–79. URL http://www.sciencedirect.com/science/article/pii/S0044848616306093

[14] Eveson J, Million J, Sardenne F, Le Croizier G (2015) Estimating growth of tropical tunas in the Indian Ocean using tag-recapture data and otolith based age estimates. Fisheries Research 163:257–272. URL http://www.sciencedirect.com/science/article/pii/S016578361400188X

[15] FAO (2018) The state of world fisheries and aquaculture. Technical report, FAO, Rome, Italy

[16] Farley J, Krusic-Golub K, Clear N, Eveson P, Smith N (2018) Progress on yellowfin tuna age and growth in the WCPO. WCPFC Project 82. In: Fourteenth Regular Session of the Scientific Committee. Busan, Republic of Korea, 8-16 August 2018, vol. WCPFC-SC14-2018/SA-WP-13, 24

[17] Farley J, Krusic-Golub K, Clear N, Eveson P, Roupsard F, Sanchez C, Smith N (2019) Progress on yellowfin tuna age and growth in the WCPO (Project 82). In: Fifteenth Regular Session of the Scientific Committee. Pohnpei, Federated States of Micronesia, 12-20 August 2019, vol. WCPFC-SC15-2019/SA-WP-03, 17

[18] Fonteneau A (1980) Croissance de l'albacore (*Thunnus albacares*) de l'Atlantique Est. Collective Volume of Scientific Papers ICCAT 9(1):152–168

[19] Fonteneau A, Chassot E (2013) An overview of yellowfin tuna growth in the Atlantic ocean: Von Bertalanffy or multistanza growth? In: ICCAT Col. Vol. Sci. Pap. ICCAT, Madrid, Spain, vol. 69(5), 2059–2075

[20] Fonteneau A, Chassot E, Bodin N (2013) Global spatio-temporal patterns in tropical tuna purse seine fisheries on drifting fish aggregating devices (DFADs): Taking a historical perspective to inform current challenges. Aquatic Living Resources 26(1):37–48. URL http://www.alr-journal.org/10.1051/alr/2013046

[21] Freitas V, Cardoso JFMF, Lika K, Peck MA, Campos J, Kooijman SALM, van der Veer HW (2010) Temperature tolerance and energetics: a dynamic energy budget-based comparison of North Atlantic marine species. Philosophical Transactions of the Royal Society B: Biological Sciences 365(1557):3553–3565. URL http://rstb.royalsocietypublishing.org/content/365/1557/3553

[22] Gaertner D, Pagavino M (1992) Observations sur la croissance de l'albacore (*Thunnus albacares*) dans l'Atlantique Ouest. Collective Volume of Scientific Papers ICCAT 36:479–505

[23] Gascuel D, Fonteneau A, Capisano C (1992) Modélisation d'une croissance en deux stances chez l'albacore (*Thunnus albacares*) de l'Atlantique Est. Aquatic Living Resources 5(3):155–172. URL https://www.cambridge.org/core/journals/aquatic-living-resources/article/

modelisation-dune-croissance-en-deux-stances-chez-lalbacore-thunnus-albacares-de-latlantique-es
0249D9A998565CDD63467D0BBC641836#

[24] Gelman A, Rubin D (1992) Inference from iterative simulation using multiple sequences. Statistical Science 7(4):457–511

[25] Hallier J, Gaertner D (2008) Drifting fish aggregation devices could act as an ecological trap for tropical tuna species. Marine Ecology Progress Series 353:255–264. URL http://www.int-res.com/abstracts/meps/v353/

[26] Hansen MJ, Boisclair D, Brandt SB, Hewett SW, Kitchell JF, Lucas MC, Ney JJ (1993) Applications of bioenergetics models to fish ecology and management: Where do we go from here? Transactions of the American Fisheries Society 122(5):1019–1030. URL http://dx.doi.org/10.1577/1548-8659(1993)122<1019:AOBMTF>2.3.CO;2

[27] ICCAT (2019) Report of the 2019 ICCAT yellowfin tuna stock assessment meeting. ICCAT, Grand-Bassam, Cote d'Ivoire, 8-16 July 2019, 117p. URL https://www.iccat.int/Documents/SCRS/DetRep/YFT_SA_ENG.pdf

[28] IOTC (2018) Report of the 21st Session of the IOTC Scientific Committee. IOTC-2018-SC21-RE_Rev1, FAO, Mahé, Seychelles, 3-7 December 2018

[29] Itano DG (2000) The reproductively biology of yellowfin tuna (*Thunnus albacares*) in Hawaiian waters and the Western Tropical Pacific Ocean: Project Summary. SOEST 00-01, JIMAR Contribution 00-328

[30] Jaquemet S, Potier M, Ménard F (2011) Do drifting and anchored Fish Aggregating Devices (FADs) similarly influence tuna feeding habits? A case study from the western Indian Ocean. Fisheries Research 107(1–3):283–290. URL http://www.sciencedirect.com/science/article/pii/S0165783610002961

[31] Jusup M, Klanjscek T, Matsuda H, Kooijman SALM (2011) A full lifecycle bioenergetic model for bluefin tuna. PLoS ONE 6(7):e21903. URL http://dx.doi.org/10.1371/journal.pone.0021903

[32] Kaji T, Tanaka M, Oka M, Takeuchi H, Ohsumi S, Teruya K, Hirokawa J (1999) Growth and morphological development of laboratory-reared yellowfin tuna *Thunnus albacares* larvae and early juveniles, with special emphasis on the digestive system. Fisheries science 65(5):700–707. URL https://www.jstage.jst.go.jp/article/fishsci1994/65/5/65_5_700/_article/-char/ja/

[33] Klinger DH, Dale JJ, Gleiss AC, Brandt T, Estess EE, Gardner L, Machado B, Norton A, Rodriguez L, Stiltner J, Farwell C, Block BA (2016) The effect of temperature on postprandial metabolism of yellowfin tuna (Thunnus albacares). Comparative Biochemistry and Physiology Part A: Molecular & Integrative Physiology 195:32–38. URL http://www.sciencedirect.com/science/article/pii/S1095643316000076

[34] Kolody DS, Eveson JP, Hillary RM (2016) Modelling growth in tuna RFMO stock assessments: Current approaches and challenges. Fisheries Research 180:177–193. URL http://www.sciencedirect.com/science/article/pii/S0165783615300035

[35] Kooijman S (2010) Dynamic Energy Budget Theory for Metabolic Organisation. Cambridge University Press

[36] Lehodey P, Leroy B (1999) Age and growth of yellowfin tuna (*Thunnus albacares*) from the western and central Pacific Ocean as indicated by daily growth increments and tagging data. 12th Meeting of the SCTB, Working Paper YFT-2 :1–21

[37] Lorenzen K (2016) Toward a new paradigm for growth modeling in fisheries stock assessments: Embracing plasticity and its consequences. Fisheries Research 180:4–22. URL http://www.sciencedirect.com/science/article/pii/S0165783616300066

[38] Magnuson J (1973) Comparative study of adaptations for continuous swimming and hydrostatic equilibrum of Scombroid and Xiphoid fishes. Fishery Bulletin 71(2):337–356

[39] Maldeniya R (1996) Food consumption of yellowfin tuna, *Thunnus albacares*, in Sri Lankan waters. Environmental Biology of Fishes 47:101–107

[40] Margulies D, Suter JM, Hunt SL, Olson RJ, Scholey VP, Wexler JB, Nakazawa A (2007) Spawning and early development of captive yellowfin tuna (*Thunnus albacares*). Fishery Bulletin 105:249–265. URL http://fishbull.noaa.gov/1052/margulies.pdf

[41] Margulies D, Scholey VP, Wexler JB, Stein MS (2016) Chapter 5 - Research on the reproductive biology and early life history of yellowfin tuna *Thunnus albacares* in Panama. In: Benetti DD, Partridge GJ, Buentello A (eds.) Advances in Tuna Aquaculture, Academic Press, San Diego. 77–114. URL http://www.sciencedirect.com/science/article/pii/B9780124114593000047

[42] Marsac F, Lablache G (1985) Preliminary study of the growth of yellowfin estimated from purse seine data in the Western Indian Ocean. IPTP Collective volume of working documents :91–110

[43] Marsac F, Fonteneau A, Ménard F (2000) Drifting FADs used in tuna fisheries : an ecological trap ? In: Le Gall J, Cayré P, Taquet M, Pêhe Thonière et Dispositifs de Concentration de Poissons : Colloque Caraibe-Martinique, Trois-Ilets (MTK), 1999/10/15-19 (eds.) Pêche thonière et dispositifs de concentration de poissons, IFREMER, Plouzané, no. 28 in Actes de Colloques - IFREMER. 537–552

[44] Maury O (2017) Can schooling regulate marine populations and ecosystems? Progress in Oceanography 156:91–103. URL http://www.sciencedirect.com/science/article/pii/S0079661116301471

[45] Maury O, Poggiale J (2013) From individuals to populations to communities: A dynamic energy budget model of marine ecosystem size-spectrum including life history diversity. Journal of Theoretical Biology 324:52–71. URL http://www.sciencedirect.com/science/article/pii/S002251931300043X

[46] Minte-Vera C, Maunder MN, Xu H, Valero JL, Lennert-Cody CE, Aires-da Silva A (2020) Yellowfin tuna in the eastern Pacific Ocean, 2019: Benchmark assessment. IATTC, La Jolla, California (USA), 11-15 May 2020, vol. SAC-11-07, 77

[47] Morize E, Munaron JM, Hallier JP, Million J (2008) Preliminary growth studies of yellowfin and bigeye tuna (*Thunnus albacares* and *T. obesus*) in the Indian Ocean by otolith analysis. IOTC Working Party on Tropical Tunas 30:13p

[48] Murua H, Eveson JP, Marsac F (2015) The Indian Ocean Tuna Tagging Programme: Building better science for more sustainability. Fisheries Research URL http://www.sciencedirect.com/science/article/pii/S0165783614002136

[49] Ney J (1993) Bioenergetics modeling today: Growing pains on the cutting edge. Transactions of the American Fisheries Society 122:736–748. URL http://www.tandfonline.com/doi/abs/10.1577/1548-8659%281993%29122%3C0736%3ABMTGPO%3E2.3.CO%3B2

[50] Nisbet RM, Jusup M, Klanjscek T, Pecquerie L (2012) Integrating dynamic energy budget (DEB) theory with traditional bioenergetic models. Journal of Experimental Biology 215:892–902. URL http://jeb.biologists.org/cgi/doi/10.1242/jeb.059675

[51] Ortega A, Mourente G (2010) Comparison of the lipid profiles from wild caught eggs and unfed larvae of two scombroid fish: northern bluefin tuna (*Thunnus thynnus* L., 1758) and Atlantic bonito (*Sarda sarda* Bloch, 1793). Fish Physiology and Biochemistry 36:461–471. URL https://doi.org/10.1007/s10695-009-9316-8

[52] Pecoraro C, Zudaire I, Bodin N, Murua H, Taconet P, Díaz-Jaimes P, Cariani A, Tinti F, Chassot E (2017) Putting all the pieces together: integrating current knowledge of the biology, ecol-

ogy, fisheries status, stock structure and management of yellowfin tuna (*Thunnus albacares*). Reviews in Fish Biology and Fisheries 27(4):811–841. URL https://link.springer.com/article/10.1007/s11160-016-9460-z

[53] Pecquerie L, Petitgas P, Kooijman SALM (2009) Modeling fish growth and reproduction in the context of the Dynamic Energy Budget theory to predict environmental impact on anchovy spawning duration. Journal of Sea Research 62:93–105. URL http://www.sciencedirect.com/science/article/pii/S138511010900063X

[54] Pecquerie L, Johnson LR, Kooijman SALM, Nisbet RM (2011) Analyzing variations in life-history traits of Pacific salmon in the context of Dynamic Energy Budget (DEB) theory. Journal of Sea Research 66(4):424–433. URL http://www.sciencedirect.com/science/article/pii/S1385110111001006

[55] Pethybridge H, Roos D, Loizeau V, Pecquerie L, Bacher C (2013) Responses of European anchovy vital rates and population growth to environmental fluctuations: An individual-based modeling approach. Ecological Modelling 250:370–383. URL http://www.sciencedirect.com/science/article/pii/S0304380012005558

[56] Pethybridge H, Choy CA, Logan JM, Allain V, Lorrain A, Bodin N, Somes CJ, Young J, Ménard F, Langlais C, Duffy L, Hobday AJ, Kuhnert P, Fry B, Menkes C, Olson RJ (2018) A global meta-analysis of marine predator nitrogen stable isotopes: Relationships between trophic structure and environmental conditions. Global Ecology and Biogeography 27(9):1043–1055. URL https://onlinelibrary.wiley.com/doi/abs/10.1111/geb.12763

[57] Polacheck T, Eveson J, Laslett G (2004) Increase in growth rates of southern bluefin tuna (\textitThunnus maccoyii) over four decades: 1960 to 2000. Canadian Journal of Fisheries and Aquatic Sciences 61:307–322

[58] Potier M, Sabatié R, Ménard F, Marsac F (2001) Preliminary results of tuna diet studies in the west equatorial Indian Ocean. IOTC Proceedings 4:273–278

[59] Potier M, Marsac F, Lucas V, Sabatié R, Hallier JP, Ménard F (2004) Feeding partitioning among tuna taken in surface and mid-water layers: The case of yellowfin (*Thunnus albacares*) and bigeye (*T. obesus*) in the western tropical indian ocean. Western Indian Ocean Journal of Marine Science 3(1):51–62. URL https://www.ajol.info/index.php/wiojms/article/view/28447

[60] Potier M, Marsac F, Cherel Y, Lucas V, Sabatié R, Maury O, Ménard F (2007) Forage fauna in the diet of three large pelagic fishes (lancetfish, swordfish and yellowfin tuna) in the western

equatorial Indian Ocean. Fisheries Research 83:60–72. URL http://www.sciencedirect.com/science/article/pii/S0165783606003079

[61] R Development Core Team (2010) R: A Language and Environment for Statistical Computing. R Foundation for Statistical Computing, Vienna, Austria. URL http://www.R-project.org/. ISBN 3-900051-07-0

[62] Rohit P, Rammohan K (2009) Fishery and biological aspects of yellowfin tuna *Thunnus albacares* along Andhra coast, India. Asian Fisheries Science 22:235–244

[63] Roxy MK, Modi A, Murtugudde R, Valsala V, Panickal S, Kumar SP, Ravichandran M, Vichi M, Lévy M (2016) A reduction in marine primary productivity driven by rapid warming over the tropical Indian Ocean. Geophysical Research Letters 43(2):826–833. URL https://agupubs.onlinelibrary.wiley.com/doi/abs/10.1002/2015GL066979. _eprint: https://agupubs.onlinelibrary.wiley.com/doi/pdf/10.1002/2015GL066979

[64] Sardenne F, Dortel E, Le Croizier G, Million J, Labonne M, Leroy B, Bodin N, Chassot E (2015) Determining the age of tropical tunas in the Indian Ocean from otolith microstructures. Fisheries Research 163:44–57. URL http://www.sciencedirect.com/science/article/pii/S0165783614000903

[65] Sardenne F, Bodin N, Chassot E, Amiel A, Fouché E, Degroote M, Hollanda S, Pethybridge H, Lebreton B, Guillou G, Ménard F (2016) Trophic niches of sympatric tropical tuna in the Western Indian Ocean inferred by stable isotopes and neutral fatty acids. Progress in Oceanography 146:75–88. URL http://www.sciencedirect.com/science/article/pii/S0079661115300641

[66] Schaefer KM, Fuller DW, Block BA (2011) Movements, behavior, and habitat utilization of yellowfin tuna (*Thunnus albacares*) in the Pacific Ocean off Baja California, Mexico, determined from archival tag data analyses, including unscented Kalman filtering. Fisheries Research 112(1):22–37. URL http://www.sciencedirect.com/science/article/pii/S016578361100275X

[67] Schaefer M, Chatwin B, Broadhead G (1961) Tagging and recovery of tropical tunas. Technical report 5, IATTC, La Jolla, California (USA)

[68] Shadwick RE, Schiller LL, Fudge DS (2013) Physiology of swimming and migration in tunas. In: Swimming Physiology of Fish, Palstra, Arjan P. and Planas, Josep V. Springer edn., 45–78

[69] Shuford R, Dean J, Stéquert B, Morize E (2007) Age and growth of yellowfin tuna in the Atlantic Ocean. Collection Volume Scientific Paper ICCAT 60(1):330–341

[70] Sousa Tânia, Domingos Tiago, Kooijman SALM (2008) From empirical patterns to theory: a formal metabolic theory of life. Philosophical Transactions of the Royal Society B: Biological Sciences 363(1502):2453–2464. URL https://royalsocietypublishing.org/doi/abs/10.1098/rstb.2007.2230

[71] Spiegelhalter D, Thomas A, Best N, Lunn D (2011) OpenBUGS version 3.2.1 user manual. Tech. rep.

[72] Stéquert B (1995) Détermination de l'âge des thons tropicaux à partir de leurs otolithes: exemple du Yellowfin (*Thunnus albacares*). Document Technique du Centre ORSTOM de Brest 76:1–31

[73] Stéquert B, Rodriguez J, Cuisset B, Le Menn F (2001) Gonadosomatic index and seasonal variations of plasma sex steroids in skipjack tuna (*Katsuwonus pelamis*) and yellowfin tuna (*Thunnus albacares*) from the Western Indian Ocean. Aquatic Living Resources 14:313–318. URL http://www.sciencedirect.com/science/article/pii/S0990744001011263

[74] Tremblay-Boyer L, McKechnie S, Pilling G, Hampton J (2017) Stock assessment of yellowfin tuna in the western and central Pacific Ocean. In: Thirteenth Regular Session of the Scientific Committee. Rarotonga, Cook Islands, 9-17 August 2017, vol. WCPFC-SC13-2017/SA-WP-06 Rev1 August 4th, 125

[75] van der Veer H, Cardoso JF, van der Meer J (2006) The estimation of DEB parameters for various Northeast Atlantic bivalve species. Journal of Sea Research 56:107–124. URL http://www.sciencedirect.com/science/article/pii/S1385110106000451

[76] Wexler JB, Scholey VP, Olson RJ, Margulies D, Nakazawa A, Suter JM (2003) Tank culture of yellowfin tuna, *Thunnus albacares*: developing a spawning population for research purposes. Aquaculture 220:327–353. URL http://www.sciencedirect.com/science/article/pii/S0044848602004295

[77] Wexler JB, Margulies D, Scholey VP (2011) Temperature and dissolved oxygen requirements for survival of yellowfin tuna, *Thunnus albacares*, larvae. Journal of Experimental Marine Biology and Ecology 404:63–72. URL http://www.sciencedirect.com/science/article/pii/S0022098111002073

[78] Wild A, Foreman T (1980) The relationship between otolith increments and time for yellowfin and skipjack tuna marked with tetracycline. Inter-American Tropical Tuna Commission Bulletin 17(7):507–560

[79] Zudaire I, Murua H, Grande M, Bodin N (2013) Reproductive potential of yellowfin tuna (*Thunnus albacares*) in the western Indian Ocean. Fishery Bulletin 111:252–264

[80] Zudaire I, Murua H, Grande M, Goñi N, Potier M, Ménard F, Chassot E, Bodin N (2015) Variations in the diet and stable isotope ratios during the ovarian development of female yellowfin tuna (*Thunnus albacares*) in the Western Indian Ocean. Marine Biology 162(12):2363–2377. URL `https://doi.org/10.1007/s00227-015-2763-0`

Figures

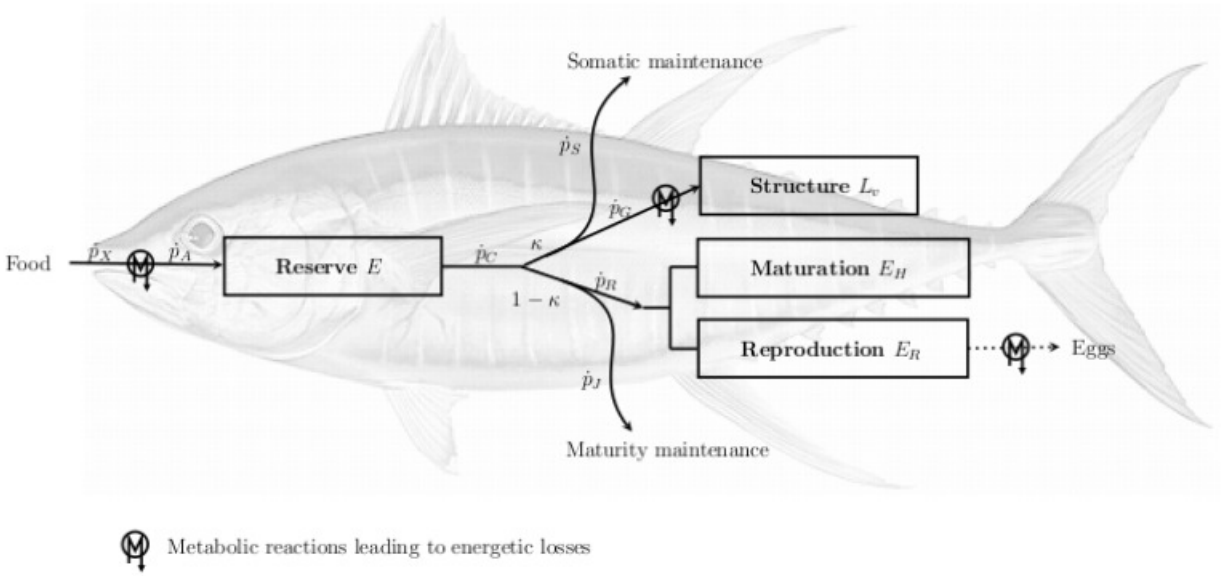

Figure 1: Conceptual representation of a Dynamic Energy Budget model for yellowfin tuna. Energy fluxes and parameters are defined in Tables 3 and 1, respectively.

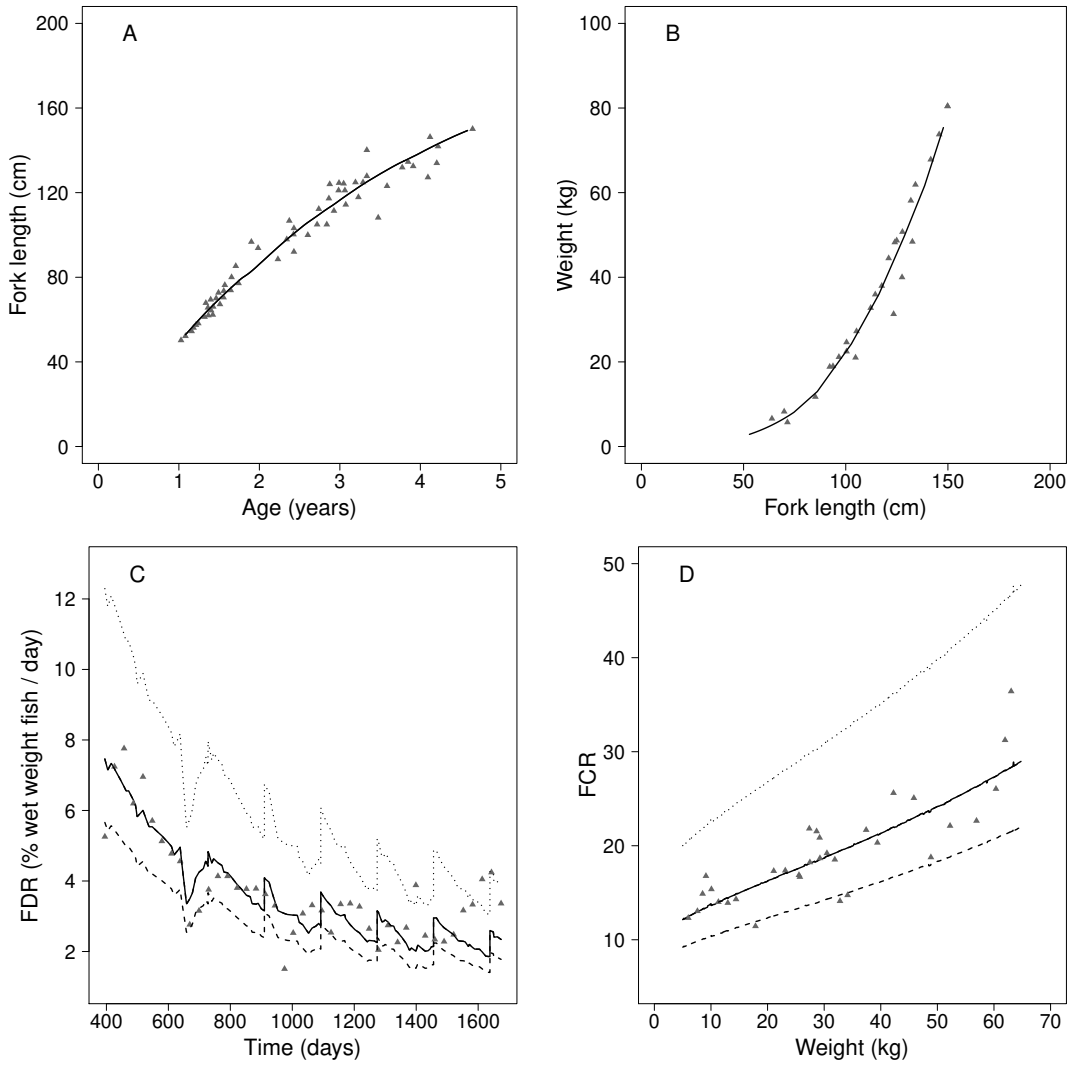

Figure 2: Comparison of simulation outputs from the DEB model with farmed yellowfin tuna data [grey triangles; 76]: growth in length (A), mean length-weight relationship (B), food daily ration (FDR, C) and food conversion ratio (FCR, D). To determine the FDR and FCR, different energetic levels of prey were used: minimal (dashed line), medium (solid line) and maximal (dotted line). Simulation was performed with a constant functional response of 0.925 and with daily body temperatures equal to the seawater temperature variations in tank (see text for details).

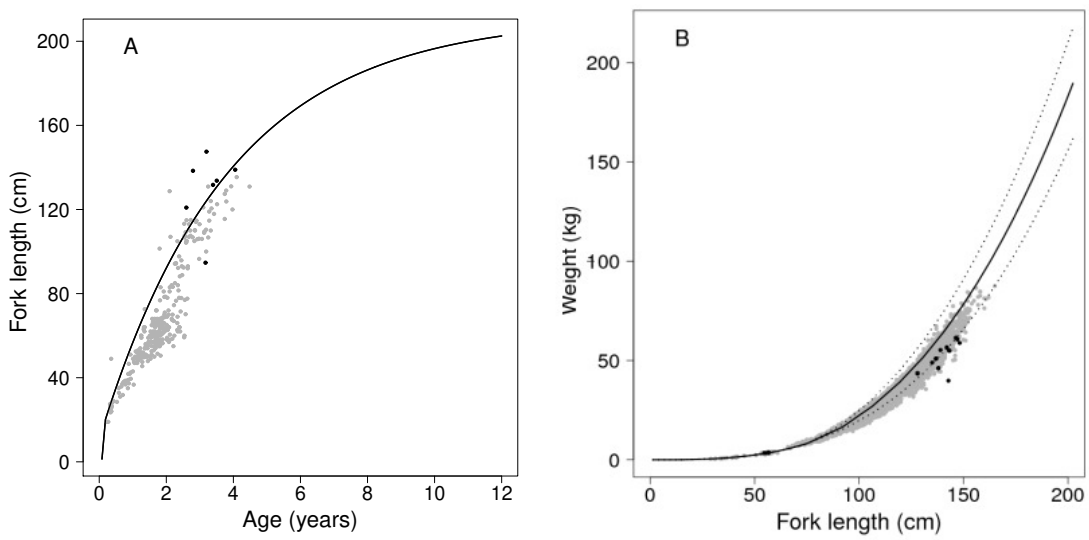

Figure 3: Comparison of yellowfin growth in length (A) and length-weight relationship (B) as simulated by the reference model in constant condition of temperature (27°C) and food density ($f = 0.925$) with data from wild yellowfin tuna of the Indian Ocean. Black circles correspond to females and grey circles to fish of indeterminate sex. In B, the solid line represents the mean length-weight relationship and the dotted lines represent the variations around this mean due to status of reproduction buffer (see text for details).

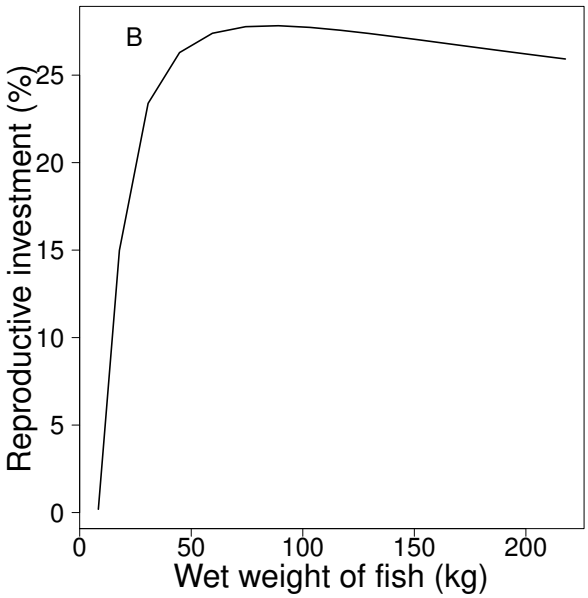

Figure 4: Seasonal reproductive investment for yellowfin tuna as simulated by the reference DEB model in constant conditions of temperature (27°C) and food density ($f = 0.925$).

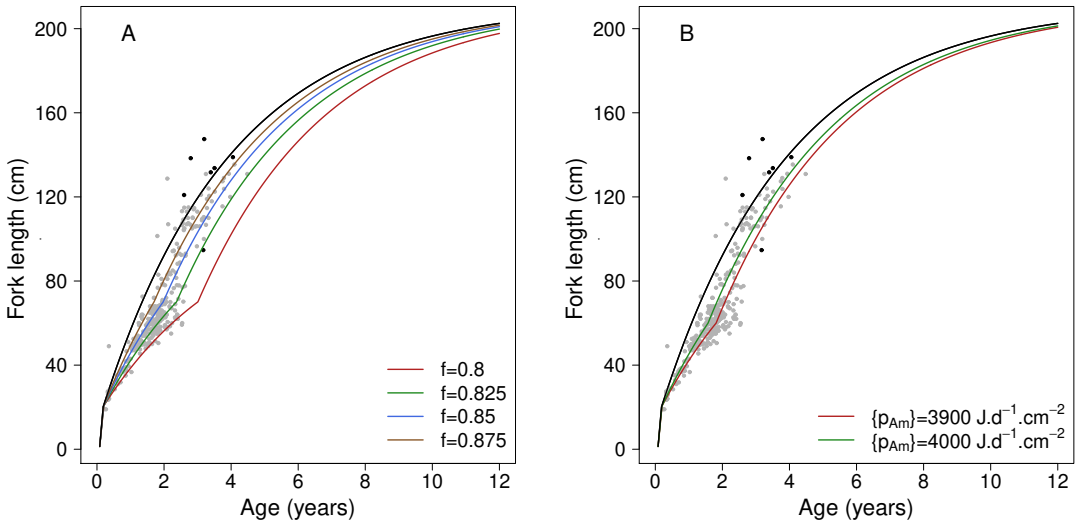

Figure 5: Simulation of yellowfin tuna growth curve under a decrease in food supply (A) and a reduced energy intake (B) in juveniles of yellowfin tuna. The black curve corresponds to the reference model and the grey circles represent the data from wild yellowfin tuna of the Indian Ocean.

Tables

Table 1: List of state variables and parameters used in DEB model. The parameters values for adult Pacific bluefin tuna [PBT; 31] and yellowfin tuna (YFT) at given for a reference temperature of 25°C.

Definition	Notation	Unit	PBT	YFT
State variables				
Scaled reserve density	e	-		
Structural length	L_V	cm		
Maturity level	E_H	J		
Reproduction buffer	E_R	J		
Primary parameters				
Fraction of mobilised reserve allocated to soma	κ	-	0.7807	0.7807
Surface-area specific maximum assimilation rate	$\{\dot{p}_{Am}\}$	$\mathrm{J.d^{-1}.cm^{-2}}$	4783.707	4370.394
Energy conductance	$\dot{v}$	$\mathrm{cm.d^{-1}}$	7.056	7.056
Volume-specific somatic maintenance rate	$[\dot{p}_M]$	$\mathrm{J.d^{-1}.cm^{-3}}$	17.395	17.395
Surface area-specific somatic maintenance rate	$\{\dot{p}_T\}$	$\mathrm{J.d^{-1}.cm^{-2}}$	2215.415	2215.415
Volume-specific costs of structure	$[E_G]$	$\mathrm{J.cm^{-3}}$	8563.387	8563.387
Maturity maintenance rate coefficient	$\dot{k}_J$	$\mathrm{d^{-1}}$	0.0612	0.0612
Maturation threshold for metamorphosis	E_H^j	J	6902.209	1368.719
Maturation threshold for end of early juvenile stage	E_H^e	J	969476	192248.7
Maturation threshold for puberty	E_H^p	J	25484395.636	5053598
Fraction of food energy fixed in reserve	κ_X	-	-	0.8
Link parameters				
Shape parameter for juvenile and adult stages	δ_j	-	0.2704	0.2559
Structural volume density	d_V	$\mathrm{g.cm^{-3}}$	1	1.0821
Weight-energy coupler	ρ_E	$\mathrm{J.g^{-1}}$	7763.975	7346.034
Arrhenius temperature	T_A	K	5298.838	4622.495
Half saturation constant	X_k	$\mathrm{J.cm^{-3}}$	0.0004463	-
Reproduction module parameters				
Energy costs of one egg	E_0	J	3.75	1.295
Fraction of reproduction energy fixed in eggs	κ_R	-	0.95	0.95
Energy density of one batch	$[E_B]$	$\mathrm{J.cm^{-3}}$	-	1.794
Compounds parameters				
Energy investment ration	g	-	$g = \frac{\dot{v}[E_G]}{\kappa\{\dot{p}_{Am}\}}$	
Structural heating length	L_T	cm	$L_T = \frac{\{\dot{p}_T\}}{[\dot{p}_M]}$	
Maximum structural length	L_m	cm	$L_m = \frac{\kappa\{\dot{p}_{Am}\}}{[\dot{p}_M]}$	
Maximum reserve density	$[E_m]$	$\mathrm{J.cm^{-3}}$	$[E_m] = \frac{\{\dot{p}_{Am}\}}{\dot{v}}$	

Table 2: Dynamics of state variables in the DEB model of yellowfin tuna.

Scaled reserve density

$$\frac{de}{dt} = (f - e)\frac{\dot{v}}{L_V} \quad \text{D1}$$

Structural length (cm)

$$\frac{dL_V}{dt} = \begin{cases} \frac{\dot{v}}{3(e+g)}\left(e - \frac{L_V}{L_m}\right) & \text{while } E_H < E_H^e \\ \frac{\dot{v}}{3(e+g)}\left(e - \frac{L_V+L_T}{L_m}\right) & \text{from } E_H \geqslant E_H^e \end{cases} \quad \text{D2}$$

Maturity level (J) while $E_H < E_H^p$

$$\frac{dE_H}{dt} = (1-\kappa) \times \frac{\{\dot{p}_{Am}\}}{e+g} \times \left(e\left(g + \frac{L_V + L_T}{L_m}\right)\right) \times L_V^2 - \dot{k}_J \times E_H \quad \text{D3}$$

Reproduction buffer (J) if $E_H \geqslant E_H^p$ **:**

$$\frac{dE_R}{dt} = \begin{cases} (1-\kappa) \times \frac{\{\dot{p}_{Am}\}}{e+g} \times \left(e\left(g + \frac{L_V+L_T}{L_m}\right)\right) \times L_V^2 - \dot{k}_J \times E_H^p - E_B & \text{if a batch is released} \\ (1-\kappa) \times \frac{\{\dot{p}_{Am}\}}{e+g} \times \left(e\left(g + \frac{L_V+L_T}{L_m}\right)\right) \times L_V^2 - \dot{k}_J \times E_H^p & \text{else} \end{cases} \quad \text{D4}$$

Table 3: Energy fluxes ($J.d^{-1}$) used in the yellowfin tuna DEB model. All parameters are defined in Table 1.

Metabolic process	Energy flux
Ingestion	$\dot{p}_X = \{\dot{p}_{Xm}\} f L_V^2 = \dfrac{\{\dot{p}_{Am}\} f L_V^2}{\kappa_X}$
Assimilation	$\dot{p}_A = \dfrac{\dot{p}_X}{\kappa_X} = \{\dot{p}_{Am}\} f L_V^2$
Mobilisation	$\dot{p}_C = [E_m] L_V^3 \left(\dfrac{\dot{v}}{L_V} + \dot{k}_M \left(\dfrac{L_V + L_T}{L_V} \right) \right) \dfrac{eg}{e+g}$
Somatic maintenance	$\dot{p}_S = \{\dot{p}_T\} L_V^2 + [\dot{p}_M] L_V^3$
Growth	$\dot{p}_G = \dfrac{\kappa \dot{p}_C - \dot{p}_S}{[E_G]}$
Maturity maintenance	$\dot{p}_J = \dot{k}_J E_H$
Maturation or reproduction	$\dot{p}_R = (1-\kappa)\dot{p}_C - \dot{p}_J$

Table 4: Mean, standard deviation (Std.dev) and credibility interval of link parameters as estimated by Bayesian inference.

Parameter	Mean	Std.dev	Posterior quantiles	
			2.5%	97.5%
δ_j	0.2559	0.0048	0.2455	0.2628
d_V	1.0821	0.0643	1.0013	1.2337
ρ_E	7346.034	136.6962	7046.95	7545.025

Table 5: Average growth rates (cm.month^{-1}) of juvenile yellowfin tuna (10-90 cm) consecutive to a decrease in food supply and reduced energy intake simulated through changes in the scaled functional response (f) and the surface-area specific maximum assimilation rate ($\{\dot{p}_{Am}\}$) respectively. The RMSE values between the average growth rates simulated and estimated for the wild Indian Ocean YFT by Dortel et al. [11] are indicated in parentheses.

Fork length	Reference	f values				$\{\dot{p}_{Am}\}$ values	
(cm)	model	0.8	0.825	0.85	0.875	3900	4000
]10,20]	14.86	12.90	13.29	13.69	14.08	13.30	13.64
]20,30]	4.12 (38.06%)	2.08 (22.69%)	2.55 (0.80%)	2.95 (13.49%)	3.34 (23.59%)	2.56 (0.79%)	2.91 (12.30%)
]30,40]	3.78 (37.30%)	1.73 (37.01%)	2.14 (10.76%)	2.55 (7.05%)	2.96 (19.93%)	2.15 (10.24%)	2.50 (5.19%)
]40,50]	3.56 (39.23%)	1.52 (42.32%)	1.93 (12.09%)	2.34 (7.55%)	2.75 (21.34%)	1.94 (11.51%)	2.28 (5.12%)
]50,60]	3.35 (41.53%)	1.30 (50.68%)	1.71 (14.55%)	2.12 (7.60%)	2.53 (22.58%)	1.72 (13.88%)	2.07 (5.37%)
]60,70]	3.13 (42.36%)	1.09 (65.51%)	1.50 (20.27%)	1.91 (5.55%)	2.32 (22.24%)	3.12 (42.18%)	3.13 (42.36%)
]70,80]	2.92 (16.08%)	2.87 (14.62%)	2.88 (14.91%)	2.89 (15.21%)	2.90 (15.50%)	2.92 (16.08%)	2.92 (16.08%)
]80,90]	2.70 (50.02%)	2.70 (50.02%)	2.70 (50.02%)	2.70 (50.02%)	2.70 (50.02%)	2.70 (50.02%)	2.70 (50.02%)